

Iterative Reed–Muller Decoding

Marvin Geiselhart*, Ahmed Elkelesh*, Moustafa Ebada*, Sebastian Cammerer† and Stephan ten Brink*

*Institute of Telecommunications, Pfaffenwaldring 47, University of Stuttgart, 70569 Stuttgart, Germany

{geiselhart,elkelesh,ebada,tenbrink}@inue.uni-stuttgart.de

†NVIDIA, Fasanenstraße 81, 10623 Berlin, Germany

scammerer@nvidia.com

Abstract—Reed–Muller (RM) codes are known for their good maximum likelihood (ML) performance in the short block-length regime. Despite being one of the oldest classes of channel codes, finding a low complexity soft-input decoding scheme is still an open problem. In this work, we present a belief propagation (BP) decoding architecture for RM codes based on their rich automorphism group. The decoding algorithm can be seen as a generalization of multiple-bases belief propagation (MBBP) using polar BP as constituent decoders. We provide extensive error-rate performance simulations and compare our results to existing decoding schemes. We report a near-ML performance for the RM(3,7)-code (e.g., 0.05 dB away from the ML bound at BLER of 10^{-4}) at a competitive computational cost. To the best of our knowledge, our proposed decoder achieves the best performance of all iterative RM decoders presented thus far.

I. INTRODUCTION

The current trend of ultra-reliable low-latency communications (URLLC) applications has urged the need for efficient short length coding schemes in combination with the availability of efficient decoders. Besides many other coding schemes, this has led to the revival of one of the oldest error-correcting codes, namely Reed–Muller (RM) codes [2], [3] – potentially also due to some existent similarities between RM codes and the newly developed family of polar codes [4], [5]. On the one hand, RM codes, as an example of algebraic codes, are known to be capacity-achieving over the Binary Erasure Channel (BEC) for a given rate [6], [7]. Moreover, and practically even more relevant, they enjoy an impressive error-rate performance under maximum likelihood (ML) decoding, which also holds in the short length regime. To this extent, several decoding algorithms have been developed in the course of RM decoding. On the other hand, to the best of our knowledge, there is still a lack of practical decoders that are characterized by near-ML performance *and* feasible decoding complexity/latency.

RM decoders can be grouped into two main categories, iterative and non-iterative decoders which we will shortly revisit in the following. In the literature, the best known decoder for RM codes over an additive white Gaussian noise (AWGN) channel is Dumer’s recursive list decoding algorithm [8], which is now known under the name SCL decoding [9], and a variant using permutations. Recently, a recursive projection-aggregation (RPA) decoding algorithm for RM codes was proposed in [10], which can be viewed as a weighted BP decoder over a redundant factor graph [11], making use of the symmetry of the RM codes (i.e., its large automorphism group). RM codes under RPA decoding were

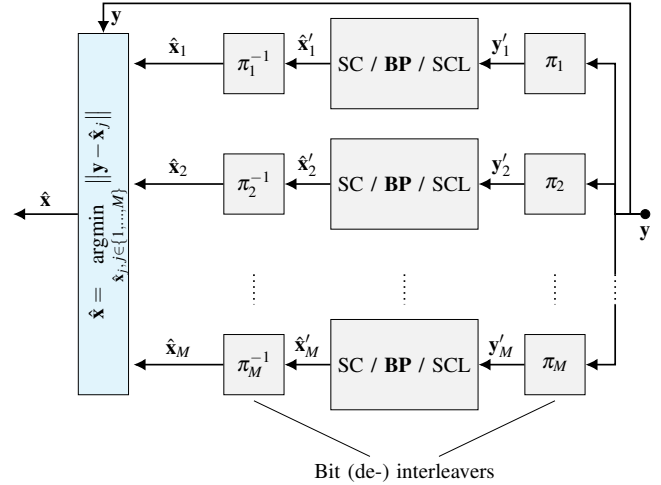


Fig. 1: Block diagram of automorphism ensemble decoding. We focus on the case where M constituent belief propagation (BP) decoders are used. The usage of successive cancellation (SC) and successive cancellation list (SCL) as constituent decoders is presented in the extended version of this paper [1].

shown to outperform the error-rate performance of CRC-aided polar codes under SCL decoding. A more general usage of the rich automorphism group of RM codes to aid the decoding process is reported in [5], along with the decoding of RM codes using a redundant parity-check matrix proposed earlier in [12]. In this work, for the sake of comparison, we consider the following iterative decoders: multiple-bases belief propagation (MBBP) decoding [13], minimum weight parity-check belief propagation (MWPC-BP) decoding [14], neural belief propagation (NBP) decoding [15], pruned neural belief propagation (pruned-NBP) decoding [16]. The inherent parallel nature of iterative decoders allows high throughput implementations. Besides, their soft-in/soft-out (SISO) nature makes them suitable for iterative detection and decoding.

In this paper, we propose a new iterative decoding scheme, extending and generalizing some of the previously mentioned decoding algorithms. To the best of our knowledge, our proposed decoding algorithm achieves the best practical iterative decoding performance of the RM(3,7)-code presented thus far (0.05 dB away from the ML bound at BLER of 10^{-4}). Fig. 1 shows an abstract view of our proposed decoding algorithm.

II. PRELIMINARIES

A. Reed–Muller Codes

We interpret each message of an RM(r,m) code as a multi-linear polynomial $u(\mathbf{z})$ in m binary variables z_j (with

An extended version of this paper is available [1].

$j \in \{0, \dots, m-1\}$) and maximum degree r , over the finite field \mathbb{F}_2 . To obtain the codeword \mathbf{x} , the message polynomial is evaluated at all points in the space \mathbb{F}_2^m , resulting in $N = 2^m$ codeword bits [2], [3].

B. Automorphism Group

The *automorphism group* (or *permutation group*) $\text{Aut}(\mathcal{C})$ of a code \mathcal{C} is the set of permutations π of the codeword bit indices that map \mathcal{C} onto itself, i.e.

$$\pi(\mathbf{x}) \in \mathcal{C} \quad \forall \mathbf{x} \in \mathcal{C} \quad \forall \pi \in \text{Aut}(\mathcal{C}), \quad (1)$$

where $\pi(\mathbf{x})$ results in the vector \mathbf{x}' with $x'_i = x_{\pi(i)}$. In other words, every codeword is mapped to another (not necessarily different) codeword of the same code. The automorphism group of RM codes is well known as the *general affine group* $\text{GA}(m)$ over the field \mathbb{F}_2 [17].¹ $\text{GA}(m)$ is the group of all affine bijections over \mathbb{F}_2^m , i.e., pairs (\mathbf{A}, \mathbf{b}) defining the mapping $\mathbf{z}' = \mathbf{A}\mathbf{z} + \mathbf{b}$, with a non-singular matrix $\mathbf{A} \in \mathbb{F}_2^{m \times m}$ and an arbitrary vector $\mathbf{b} \in \mathbb{F}_2^{m \times 1}$. The vectors $\mathbf{z}, \mathbf{z}' \in \mathbb{F}_2^{m \times 1}$ are the binary representations of the code bit positions i and $\pi(i)$, respectively, i.e., $i = \sum_{j=0}^{m-1} z_j \cdot 2^j$. An important subgroup of $\text{GA}(m)$ is the set of stage-shuffle permutations $\Pi(m)$, corresponding to the special case where \mathbf{A} is a permutation matrix and $\mathbf{b} = \mathbf{0}$.

C. Iterative RM Decoding

In this section, we briefly revise the different iterative decoding techniques which can be used for RM codes.

1) *Naïve Belief Propagation Decoding*: BP decoding can be performed over the Tanner graph of a code's parity-check matrix. However, for high-density parity-check codes like RM codes, the performance of this decoder is usually poor due to the numerous short cycles in the graph.

2) *Belief Propagation Decoding over Forney-style Factor Graph*: Rather than on a Tanner graph, BP decoding can also be performed over a Forney-style factor graph (FFG), constructed from check and variable nodes of degree three [18]. Fig. 2 shows the FFG of the RM(1,3)-code.

As the frozen nodes always contribute the same Log-likelihood ratios (LLRs) (i.e., a priori LLRs of $+\infty$) to the equations, the FFG can be reduced as shown on the right in Fig. 2, by removing edges of constant value. This potentially reduces the number of performed arithmetic operations per iteration while preserving the same performance [18]. In this work, whenever the BP decoding is used over the FFG, we use the reduced version.

3) *Minimum Weight Parity-Check Belief Propagation Decoding*: Minimum weight parity-check belief propagation (MWPC-BP) decoding introduced in [14] is based on the concept of iterative decoding over an overcomplete parity-check matrix. An online algorithm tailored to the noisy received sequence \mathbf{y} is used to construct the overcomplete parity-check matrix only based on minimum weight parity-checks.

¹In this paper, we only consider the field \mathbb{F}_2 and hence, we omit the size of the field in the notation, i.e., we write $\text{GA}(m)$ instead of $\text{GA}(m, 2)$.

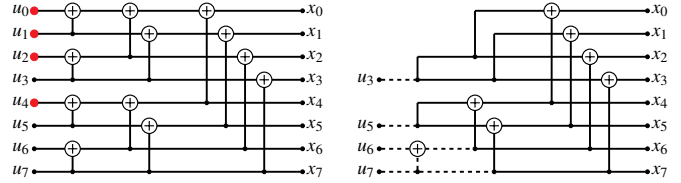


Fig. 2: Forney-style factor graph (FFG) of the RM(1,3)-code (left) and the reduced FFG (right). Note that the dashed lines indicate variables to be computed only in the right-to-left message update.

4) *Neural Belief Propagation Decoding*: Neural belief propagation (NBP) decoding as introduced in [15] treats the unrolled Tanner graph of the code as a neural network (NN), while assigning *trainable* weights to all of its edges leading to a *soft* Tanner graph. These trainable weights are optimized via stochastic gradient descent (SGD) methods.

5) *Pruned Neural Belief Propagation Decoding*: Pruned neural belief propagation (pruned-NBP) decoding [16] combines the idea of MWPC-BP together with NBP. To get started, a redundant parity-check matrix containing (all or some of) the minimum weight parity-checks is constructed. During the offline training phase, all edges connected to a check node are assigned a single trainable weight and the least contributing check nodes are *pruned* (i.e., removed) from the graph. The authors of [16] refer to this decoder as D_1 . An enhanced version, decoder D_3 , is the result of assigning trainable weights per edge at the expense of larger memory requirements to save all weights per edges. Furthermore, a pruned NBP decoder without any weights is introduced as D_2 , however with the expense of a significant degradation in error-rate performance.

III. AUTOMORPHISM ENSEMBLE DECODING

Ensemble decoding uses multiple constituent decoders (i.e., a decoder *ensemble* of size M) to generate a set of codeword estimates and selects one of these codewords, using a predefined metric, as the decoder output. Typically, a least-squares metric is used, as this corresponds to the ML decision for the AWGN channel. Hence, this method is also called *ML-in-the-list*. This can be formulated as

$$\hat{\mathbf{x}} = \underset{\hat{\mathbf{x}}_j, j \in \{1, \dots, M\}}{\operatorname{argmin}} \left\| \hat{\mathbf{x}}_j - \mathbf{y} \right\|^2 = \underset{\hat{\mathbf{x}}_j, j \in \{1, \dots, M\}}{\operatorname{argmax}} \sum_{i=0}^{N-1} \hat{x}_{j,i} \cdot y_i, \quad (2)$$

where $\hat{x}_{j,i} \in \{\pm 1\}$, $\hat{\mathbf{x}}_j$ is the estimated codeword from decoder j for the received vector \mathbf{y} and $\hat{\mathbf{x}}$ is the final codeword estimate of the ensemble.

MBBP is a well-known example for ensemble decoding that uses M BP decoders, each based on a different random parity-check matrix [13]. Another instance of ensemble decoding is belief propagation list (BPL) decoding of polar codes, where the stages of the FFG are randomly permuted for each constituent decoder [19].

In this work, we propose *automorphism ensemble BP decoding* (Aut- M -BP) for RM codes. The main idea is to make use of the already existent polar BP decoder. Furthermore, we use the RM code symmetry in the decoding algorithm itself, as permuting a valid RM codeword with a permutation from

the code’s automorphism group results in another valid RM codeword.

An abstract view of our proposed Aut- M -BP decoding algorithm is shown in Fig. 1. The input to the decoder is the received noisy codeword \mathbf{y} . We randomly sample M different permutations from the RM automorphism group, where each permutation is denoted by π_j , with j being the decoder index and $j \in \{1, 2, \dots, M\}$. The \mathbf{y} -vector is interleaved (i.e., permuted) with the M different permutations π_j leading to M permuted noisy codewords \mathbf{y}'_j , where $j \in \{1, 2, \dots, M\}$. Now we decode every \mathbf{y}'_j -vector independently using BP, whose output is the interleaved estimated codeword $\hat{\mathbf{x}}'_j$. A de-interleaving phase is applied to all M interleaved estimated codewords $\hat{\mathbf{x}}'_j$ and, thus, we have M codeword estimates $\hat{\mathbf{x}}_j$. Let $\text{BP}(\cdot)$ denote the BP decoding function that maps \mathbf{y}'_j to $\hat{\mathbf{x}}'_j$. Then we can write the interleaved decoding as

$$\hat{\mathbf{x}}_j = \pi_j^{-1}(\text{BP}(\pi_j(\mathbf{y}))). \quad (3)$$

Similar to MBBP and BPL decoding, our proposed decoding algorithm uses the *ML-in-the-list* picking rule according to Eq. (2) to choose the most likely codeword from the list to get the final decoder output $\hat{\mathbf{x}}$.

As the decoders are linear, their decoding behavior is only dependent on the noise induced by the channel, and not the choice of the transmitted codeword. Therefore, decoding using automorphisms according to Eq. (3) corresponds to permuting the *noise*. It is reasonable to conclude that suboptimal (i.e., not ML) decoders may react differently to noise realizations in different permutations, which is exactly the property that automorphism ensemble decoding seeks to exploit.

Our proposed algorithm can be therefore seen as a natural generalization of the BPL decoder [19]: We still use M parallel independent BP decoders. However, we use a more general set of permutations. It was shown in [20] that the stage-shuffling of the FFG is equivalent to a bit-interleaving operation while keeping the factor graph unchanged; these permutations correspond to the automorphism subgroup $\Pi(m)$. In contrast, we use permutations from the whole RM code automorphism group $\text{GA}(m)$ (rather than only $\Pi(m)$, which is used in BPL decoding as proposed in [19]).

It is worth mentioning that the usage of a BP decoder as a constituent decoder has some similarities when compared to *automorphism group decoding* of Bose-Chaudhuri-Hocquenghem (BCH) and Golay codes for the BEC [21] and for the AWGN channel [22]. Automorphism group decoding is based on permuting the received sequence exploiting automorphisms of the code while applying an iterative message passing algorithm.

IV. RESULTS

Regarding practical applications, both error-rate performance and the computational complexity of the decoding scheme have to be considered. We compare the described decoding schemes for the RM(3,7)-code with $N = 128$ and $k = 64$. In the following, we specify the parameters of some of the compared decoders for reproducibility:

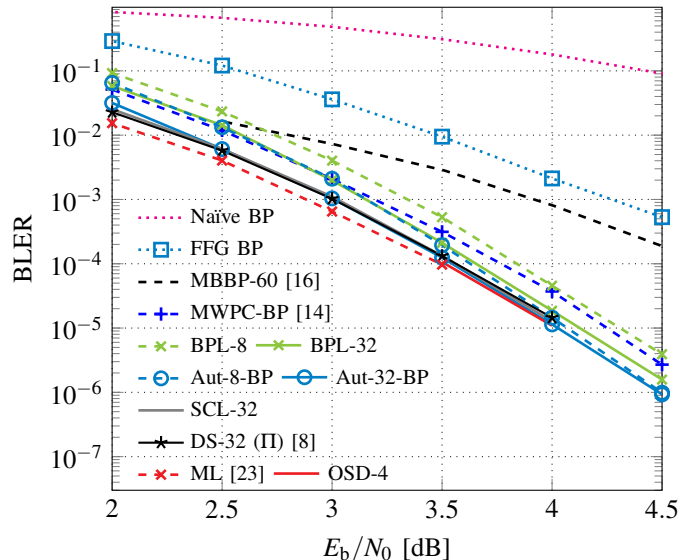


Fig. 3: BLER comparison between non SGD-optimized iterative decoders, recursive list decoding and our proposed Aut-BP decoding scheme for the RM(3,7)-code over the BI-AWGN channel.

- **MWPC-BP** utilizes 5% of the minimum-weight parity-checks, as reported in [14].
- **MBBP** operates over $M = 60$ randomly generated parity-check matrices with 6 iterations each.
- **Neural-BP** uses all 94488 minimum-weight parity-checks over 6 iterations.
- The **pruned neural-BP** employs on average 3% of the minimum-weight parity-checks over a total of 6 iterations. We consider the three variants of this decoder as introduced in [16], with tied weights (D_1), no weights (D_2) and free weights (D_3).
- For our proposed **Aut-BP**, we show results for both $M = 8$ and $M = 32$ randomly chosen permutations from the full automorphism group. Here, up to $N_{\text{it,max}} = 200$ iterations are performed with, however, an early stopping condition (i.e., when $\hat{\mathbf{x}} = \hat{\mathbf{u}}\mathbf{G}$) employed to reduce the average total number of iterations. Furthermore, the FFGs have been reduced from 1792 to 1334 box-plus and addition operations per full iteration by removing operations with constant results, as presented in Section II-C2.

A. Error-Rate Performance

In Fig. 3 and Fig. 4, we showcase the error-rate performance of the described decoding schemes for the RM(3,7)-code over the AWGN channel using binary phase shift keying (BPSK) mapping. Furthermore, we show the ML performance of the code as provided by [23]. As no data beyond an signal-to-noise-ratio (SNR) of 3.5 dB is available, the ML performance is estimated using order-4 ordered statistic decoding (OSD).

Fig. 3 compares the non-SGD-optimized iterative decoders with Aut-BP and ML. One can observe that the naïve BP decoding suffers from a very poor performance for RM codes, compared to BP decoding over FFG. Moreover, using multiple \mathbf{H} -matrices in MBBP leads to a significant enhancement in performance. All of the previous methods are outperformed

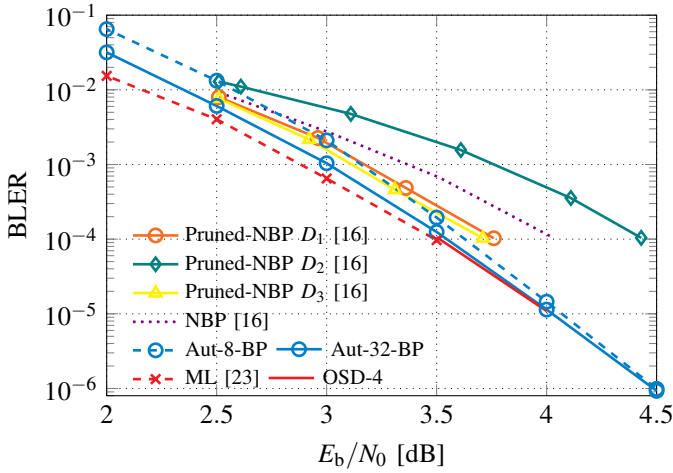


Fig. 4: BLER comparison between SGD-optimized (NN-based) iterative decoders and Aut-BP for the RM(3,7)-code over the BI-AWGN channel. All neural-BP decoders use $N_{it} = 6$ iterations.

by both Aut-8-BP and MWPC-BP, with similar performance. However, in the high SNR regime, Aut-8-BP beats MWPC-BP by 0.2 dB. Aut-32-BP even closes the gap to ML to less than 0.05 dB at a block error rate (BLER) of 10^{-4} . We further observe the gains of sampling from $GA(m)$ in Aut-BP compared to $\Pi(m)$, as used in BPL decoding. We can see that for all ensemble sizes M , sampling from $GA(m)$ consistently outperforms $\Pi(m)$ by up to 0.3 dB. This confirms the sub-optimality of restricting the automorphisms to a small subgroup. Moreover, Aut-32-BP can even outperform SCL [9] with list size $L = 32$ (i.e., SCL-32) and its permutation variant DS-32 [8] in the high SNR regime.

Fig. 4 compares the SGD-optimized (NN-based) decoders with Aut-BP and ML. Here, the neural-BP decoder is much closer to the ML bound, and the pruned variant with free weights D_3 outperforms NBP, which uses all overcomplete parity-checks. The pruned NBP D_2 decoder without weights suffers from a significant performance degradation. Over the whole SNR range, D_1 and D_3 are outperformed by Aut-32-BP. Furthermore, it can be seen that using only $M = 8$ parallel BP decoders (i.e., Aut-8-BP) results in a small performance degradation of less than 0.2 dB over the whole SNR range, offering an attractive trade-off for lower complexity. Simulation results for the RM(4,8)-code are presented in [1].

B. Iterative Decoding Complexity

For the RM(3,7)-code, we compare the complexity of the iterative decoding algorithms with error-rate performance close to ML by counting the number of computing operations required to decode one RM codeword. The first column of Table I gives the list of the operations we use.² Furthermore, as non-trivial multiplication is significantly more complex than the other considered operations, we introduce a weighting factor for multiplication $w_{mul} = 3$ (equivalent to the number of full-adders in a 4+1 bit fixed-point implementation) to make

²Note that these operations differ from the ETSI basic operations, as we are more interested in hardware than in software implementations.

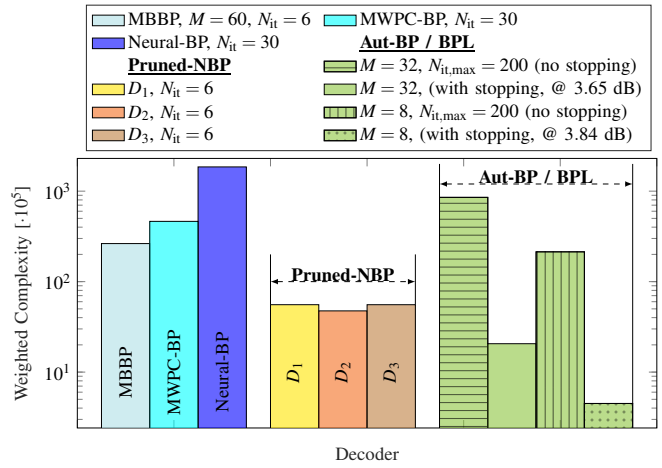


Fig. 5: Complexity comparison of different iterative decoders using basic operations weighted according to Table I (e.g., weight for multiplication = 3) to reach a target BLER of 10^{-4} ; RM(3,7)-code; BI-AWGN channel.

the comparison more fair. For all decoders, we assume that the box-plus operation is implemented as

$$L_1 \boxplus L_2 = \text{sgn}(L_1) \cdot \text{sgn}(L_2) \cdot \min(|L_1|, |L_2|) + f_+(|L_1 + L_2|) - f_+(|L_1 - L_2|), \quad (4)$$

where $f_+(|x|) = \log(1 + \exp(-|x|))$ is a correction term that can be well-approximated by a short look-up table (LUT). Furthermore, check nodes (CNs) are assumed to be efficiently implemented using the box-minus operator as

$$L_{j \rightarrow i} = \boxminus_{i' \neq i} L_{i' \rightarrow j} = \left(\boxplus_{i'} L_{i' \rightarrow j} \right) \boxminus L_{i \rightarrow j}, \quad (5)$$

with $L_1 \boxminus L_2 = \text{sgn}(L_2) \cdot L_1 + f_-(|L_1 + L_2|) - f_-(|L_1 - L_2|)$ and $f_-(|x|) = \log(1 - \exp(-|x|))$ which is again implemented as a LUT as proposed in [24]. The remaining columns of Table I list the number of operations of each type required for the basic building blocks of the described iterative decoding algorithms, namely box-plus evaluations, CN and variable node (VN) updates, the ML-in-the-list decision and the stopping condition that is used in BPL decoding. Neural-BP, the pruned neural-BP and MWPC-BP decoding use non-trivial multiplications with the corresponding weights before the VN evaluations.

Fig. 5 shows the total number of weighted operations to decode one codeword of the RM(3,7)-code. We can see that out of all methods, neural-BP using the full overcomplete \mathbf{H} -matrix has the highest complexity. The corresponding pruned decoders D_1 and D_3 result in approximately 3% of that complexity. MWPC-BP is computationally more expensive, as it uses more parity-check equations and more iterations are required to achieve a good error-rate performance. It has to be noted, however, that we only list the complexity of iterative decoding, not of (adaptively) obtaining the parity-check equations. Hence, the overall complexity of MWPC-BP is higher than the presented number. MBBP has roughly half the complexity of MWPC-BP, while Aut-32-BP without stopping condition has twice the complexity of MWPC-BP. However, when a (\mathbf{G} -matrix-based) stopping condition is used,

Table I: Basic operations and their usage in iterative decoding. ^aFor BP with weights (MWPC-BP, NBP, D1, D3).

Operation	Weight	2-input \boxplus	CN (deg. D)	VN (deg. D)	ML out of M	FFG BP Stopping
$\text{sgn}(x) \cdot \text{sgn}(y)$	1	1	$D-1$	0	0	$m \cdot N/2 + 2N - 1$
$\text{sgn}(x) \cdot y$	1	1	$2D-1$	0	MN	0
$\min(x , y)$	1	1	$D-1$	0	0	0
$\max(x, y)$	1	0	0	0	$M-1$	0
$f_{\pm}(x)$ (LUT)	1	2	$4D-2$	0	0	0
$x+y, x-y$	1	4	$8D-4$	$2D$	$M(N-1)$	0
$x \cdot y$	3	0	0	$[D+1]^a$	0	0
Weighted total	-	9	$16D-9$	$2D [+3D + 3]^a$	$2MN-1$	$m \cdot N/2 + 2N - 1$

the average number of iterations of Aut-BP is significantly reduced. To illustrate this, we measure the average required number of iterations until convergence for both $M = 8$ and $M = 32$ with respect to the SNR of the AWGN channel, while $N_{\text{it,max}} = 200$. At an SNR of 3.65 dB, corresponding to the BLER of 10^{-4} , each decoder of the Aut-32-BP ensemble requires an average of 4.55 iterations, making Aut-BP the least complex decoder of the compared algorithms (see Fig. 5), without losing any error-rate performance. Aut-8-BP requires an SNR of 3.84 dB to reach this BLER performance, however, reducing the complexity again by a factor of 4, using only 3.96 iterations on average. Note that even though the ML-in-the-list decision can be only made after all constituent decoders are terminated, terminated decoders can already start decoding the next received vector (e.g., in a super-scalar implementation).

It is also worth noting here that the approaches proposed in [16] can also profit from early stopping. However, the effect is less significant since the majority of check node evaluations are performed in the first two iterations. Moreover, the regular structure of the FFG may result in more preferable implementations of Aut-BP compared to the random memory access patterns observed in conventional iterative decoders.

V. CONCLUSION

In this work, we propose an automorphism-based iterative decoding algorithm for RM codes. We present near-ML error-rate performance for the RM(3,7)-code operating only 0.05 dB away from the ML bound at BLER of 10^{-4} . Furthermore, we report a decoder complexity comparison for the RM(3,7)-code from an operation level perspective. To the best of our knowledge, our proposed iterative Aut-BP decoders using the RM code automorphism group as permutations are the best iterative decoders reported in literature thus far in terms of error-rate performance.

REFERENCES

- [1] M. Geiselhart, A. Elkelesh, M. Ebada, S. Cammerer, and S. ten Brink, "Automorphism Ensemble Decoding of Reed-Muller Codes," *IEEE Trans. Commun.*, 2021.
- [2] D. E. Muller, "Application of Boolean Algebra to Switching Circuit Design and to Error Detection," *Transactions of the I.R.E. Professional Group on Electronic Computers*, vol. EC-3, no. 3, pp. 6–12, 1954.
- [3] I. Reed, "A class of multiple-error-correcting codes and the decoding scheme," *Transactions of the IRE Professional Group on Information Theory*, vol. 4, no. 4, pp. 38–49, Sep. 1954.
- [4] E. Arkan, "Channel Polarization: A Method for Constructing Capacity-Achieving Codes for Symmetric Binary-Input Memoryless Channels," *IEEE Trans. Inf. Theory*, vol. 55, no. 7, pp. 3051–3073, Jul. 2009.

- [5] N. Stolte, "Rekursive Codes mit der Plotkin-Konstruktion und ihre Decodierung," Ph.D. dissertation, Technische Universität Darmstadt, Jan. 2002. [Online]. Available: <http://tuprints.ulb.tu-darmstadt.de/183/>
- [6] E. Abbe, A. Shpilka, and A. Wigderson, "Reed-Muller Codes for Random Erasures and Errors," *IEEE Trans. Inf. Theory*, vol. 61, no. 10, pp. 5229–5252, 2015.
- [7] S. Kudekar, S. Kumar, M. Mondelli, H. D. Pfister, E. Şaçoğlu, and R. Urbanke, "Reed-Muller Codes Achieve Capacity on Erasure Channels," *IEEE Trans. Inf. Theory*, vol. 63, no. 7, pp. 4298–4316, 2017.
- [8] I. Dumer and K. Shabunov, "Soft-Decision Decoding of Reed-Muller Codes: Recursive Lists," *IEEE Trans. Inf. Theory*, vol. 52, no. 3, pp. 1260–1266, Mar. 2006.
- [9] I. Tal and A. Vardy, "List Decoding of Polar Codes," *IEEE Trans. Inf. Theory*, vol. 61, no. 5, pp. 2213–2226, May 2015.
- [10] M. Ye and E. Abbe, "Recursive projection-aggregation decoding of Reed-Muller codes," *IEEE Trans. Inf. Theory*, pp. 1–1, 2020.
- [11] M. Lian, C. Häger, and H. D. Pfister, "Decoding Reed-Muller Codes Using Redundant Code Constraints," in *IEEE Inter. Symp. Inf. Theory (ISIT)*, Jun. 2020.
- [12] M. Bossert and F. Hergert, "Hard- and Soft-Decision Decoding Beyond the Half Minimum Distance—An Algorithm for Linear Codes," *IEEE Trans. Inf. Theory*, vol. 32, no. 5, pp. 709–714, 1986.
- [13] T. Hehn, J. B. Huber, S. Laendner, and O. Milenkovic, "Multiple-Bases Belief-Propagation for Decoding of Short Block Codes," in *IEEE Inter. Symp. Inf. Theory (ISIT)*, Jun. 2007, pp. 311–315.
- [14] E. Santi, C. Häger, and H. D. Pfister, "Decoding Reed-Muller Codes Using Minimum-Weight Parity Checks," in *IEEE Inter. Symp. Inf. Theory (ISIT)*, Jun. 2018, pp. 1296–1300.
- [15] E. Nachmani, E. Marciano, L. Lugosch, W. J. Gross, D. Burshtein, and Y. Be'ery, "Deep Learning Methods for Improved Decoding of Linear Codes," *IEEE J. Sel. Topics Sig. Process.*, vol. 12, no. 1, pp. 119–131, Feb. 2018.
- [16] A. Buchberger, C. Häger, H. D. Pfister, L. Schmalen, and A. G. i Amat, "Pruning Neural Belief Propagation Decoders," in *IEEE Inter. Symp. Inf. Theory (ISIT)*, Jun. 2020.
- [17] F. J. MacWilliams and N. J. A. Sloane, *The Theory of Error-Correcting Codes*, ser. North-Holland Mathematical Library. North-Holland Pub. Co., 1977, no. 16.
- [18] G. D. Forney, "Codes on Graphs: Normal Realizations," *IEEE Trans. Inf. Theory*, vol. 47, no. 2, pp. 520–548, Feb. 2001.
- [19] A. Elkelesh, M. Ebada, S. Cammerer, and S. ten Brink, "Belief Propagation List Decoding of Polar Codes," *IEEE Commun. Lett.*, vol. 22, no. 8, pp. 1536–1539, Aug. 2018.
- [20] N. Doan, S. A. Hashemi, M. Mondelli, and W. J. Gross, "On the Decoding of Polar Codes on Permuted Factor Graphs," in *IEEE Global Commun. Conf. (GLOBECOM)*, Dec. 2018.
- [21] T. Hehn, O. Milenkovic, S. Laendner, and J. B. Huber, "Permutation Decoding and the Stopping Redundancy Hierarchy of Cyclic and Extended Cyclic Codes," *IEEE Trans. Inf. Theory*, vol. 54, no. 12, pp. 5308–5331, 2008.
- [22] I. Dimnik and Y. Be'ery, "Improved Random Redundant Iterative HDPC Decoding," *IEEE Trans. Commun.*, vol. 57, no. 7, pp. 1982–1985, Jul. 2009.
- [23] M. Helmling, S. Scholl, F. Gensheimer, T. Dietz, K. Kraft, S. Ruzika, and N. Wehn, "Database of Channel Codes and ML Simulation Results," www.uni-kl.de/channel-codes, 2019.
- [24] T. Clevorn and P. Vary, "The box-minus operator and its application to low-complexity belief propagation decoding," in *IEEE 61st Veh. Technol. Conf.*, vol. 1, May 2005, pp. 687–691.